PROPAGATION VELOCITY OF EXTREMELY HIGH FREQUENCY MAGNETOPLASMA WAVES IN BISMUTH

V. S. ÉDEL'MAN

Institute of Physics Problems, USSR Academy of Sciences

Submitted February 8, 1968

Zh. Eksp. Teor. Fiz. 54, 1726–1737 (June, 1968)

The velocities of magnetoplasma S and P waves in bismuth are measured at frequencies between 9 and 36 GHz at magnetic field strengths for which there is no time or space dispersion. The measurements are performed for three directions in the wave vector **k**, namely parallel to the trigonal, binary, or bissector axis, and for a field H rotating in planes both perpendicular and parallel to **k**. A deviation of the $k(H^{-1})$ dependence from linearity is detected for P waves at small values of cos ϑ, and an explanation for this deviation is proposed. The results of the measurements are compared with the theory and with the results of other experimental investigations.

INTRODUCTION

THE phenomenon of propagation of weakly damped electromagnetic waves in bismuth situated in a strong magnetic field was investigated by many both experimentally[1-8] and theoretically[2,9,10]. The main properties of these waves can be regarded as investigated with sufficient detail. However, in a comparison of the numerical values of the constants characterizing the propagation of the waves, appreciable disparities are observed between the different experimental results. At the same time, apparently, there are no grounds for expecting the theory employed in a comparison of results of experiments performed at different frequencies[1-8] to require any modification, all the more since it is constructed on the basis of the kinetic equation, Maxwell's equations, and the notion of quasiparticles (electrons and holes) in a metal, i.e., premises which are among the most general in physics. It is therefore necessary to clarify the reasons for the disagreement between the values of the velocity of the magnetoplasma waves in bismuth, obtained at different frequencies.

To this end, thorough measurements were made of the velocity of magnetoplasma waves at different directions of **H** and **k** relative to the bismuth crystal axis in the frequency range 9–36 GHz, and a comparison was made of the results of our experiments with the results of experiments by others[4-8]. Special care was taken to satisfy in the experiment the premises on which the derivation of the asymptotic relations between ω, **H**, and **k** for magnetoplasma waves is based in experiment. Such an analysis, insofar as we know, has not been performed to date.

The results of the experiments are compared also with the calculated values of the wave velocities when H and k are directed along the symmetry axes of Bi. The calculation was performed with the ellipsoidal model of the Fermi surface with parameters obtained in experiments on cyclotron resonance[11], cyclotron resonance cutoff[12], and quantum oscillations[13,14].

1. THEORY

We consider briefly the main theoretical results obtained in[2,9,10] and also certain necessary additional considerations.

1.1. In strong fields there can propagate in bismuth waves of two types, called in[1] S and P waves. They are also called fast-magnetosonic and Alfven waves, respectively[10]. If the conditions

$$\left(\frac{\omega}{\Omega}\right)^2 \ll 1, \quad \left(\frac{kV_F}{\omega}\right)^2 \approx \left(\frac{\overline{V}_F}{v}\right)^2 \ll 1, \quad \left(\frac{\pi d}{\lambda}\right)^2 \ll 1 \qquad (1)$$

are satisfied (ω—angular frequency of the wave, Ω—characteristic cyclotron frequency, **k**—wave vector, $\overline{V}_F$—carrier drift velocity, v—phase velocity of the wave, d—diameter of cyclotron orbit, and λ—wavelength in Bi), i.e., in the absence of spatial or temporal dispersion, the waves have the following properties:

The S wave has a spectrum $\omega \propto kH$ and exists for all angles $\vartheta = \sphericalangle(\mathbf{k}, \mathbf{H}) = \sphericalangle(\mathbf{N}, \mathbf{H})$ (**N**—normal to the surface of the sample; for magnetoplasma waves we always have $\mathbf{N} \parallel \mathbf{k}$, since $v/c \ll 1$[2]). When $\vartheta \approx \pi/2$, its electric field **E** (or high frequency current **J**) is perpendicular to the plane containing the vectors **H** and **k**.

In the case of small cos ϑ and when the condition $(\omega\Omega^{-1} \tan\vartheta)^2 \ll 1$, is satisfied, the P wave has a spectrum $\omega \propto \mathbf{k}\cdot\mathbf{H}$; when $\mathbf{k} \perp \mathbf{H}$, the P wave does not exist. When cos ϑ is small, its vector $\mathbf{E} \perp \mathbf{H}$ lies in the plane containing the vectors **H** and **k**.

When $\vartheta \ll 1$, there are no fundamental differences between the two types of waves, and the difference between their velocities and polarizations is due to the anisotropy of the Fermi surface. In particular, it follows from symmetry consideration alone that when[1)] $\mathbf{H} \parallel \mathbf{k} \parallel C_3$ the polarization of the wave in the metal coincides with the polarization of the incident wave and its velocity does not depend on the polarization.

1.2. It is clear from the form of the wave spectrum

[1)]We use the following designations for the crystal axes: C_1—bisector, C_2—binary, C_3—trigonal.

that the phase velocity $v = \omega/k \propto H$, meaning that the ratio v/H at given directions of H and k is a constant determined by the parameters of the Fermi surface. In discussing the results of the experiments, some authors use also a quantity called the mass density, which is connected with v/H by the relation

$$[nf(m)]^{1/2} = H / 4\pi v.$$

To calculate the values of v/H as a function of H and k, we assume for the Fermi surface of bismuth a model consisting of three electronic and one hole ellipsoid. The equation of the electronic ellipsoid (in terms of the principal axes) is

$$2\varepsilon_e = \frac{p_\alpha^2}{m} + \frac{p_\beta^2}{m_\beta} + \frac{p_2^2}{m},$$

with $2\epsilon_e = 5.78 \times 10^{-14}$ erg, $m_\alpha = 1.27\, m_0$, $m_\beta = 1.15 \times 10^{-2}\, m_0$, and $m_2 = 0.57 \times 10^{-2}\, m_0$ (m_0—mass of free electron). The angle of inclination of the axis to the trigonal axis $\psi = 6°20'$ (these parameters were calculated on the basis of the results of[11-13]. For the ratio $(m_\beta/m_2)^{1/2}$ we used the mean of the ratio of the cyclotron masses on the central sections[11] and the ratio of the momenta[12].) The equation of the hole ellipsoid is

$$2\varepsilon_h = \frac{P_1^2}{M_1} + \frac{P_2^2}{M_2} + \frac{P_3^2}{M_3},$$

where $2\epsilon_h = 3.75 \times 10^{-14}$ erg, $M_1 = M_2 = 0.063 m_0$, and $M_3 = 0.65 m_0$ (the parameters were calculated from the values of the effective masses[11] and the extremal cross section at $H \parallel C_3$[14].)

1.3. With the aid of formulas (7), (13), and (14) of[2] we can calculate the asymptotic S- and P-wave velocities corresponding to the conditions (1). We shall not present here the corresponding calculations, which are known from a number of papers (for example,[5,7]). The numerical values of v/H, obtained for H and k directed along the axes C_1, C_2 or C_3, are listed in the table[2)]. Allowance for the temporal or spatial dispersion leads to the appearance of additions to the components of the conduction tensor on the order of $(\omega/\Omega)^2$, $(\mathbf{k}\cdot\overline{\mathbf{v}}_F/\omega)^2$, $(\mathbf{k}\cdot\overline{\mathbf{v}}_F/\Omega)^2$, or $(\pi d/\lambda)^2$; this can result in additions of the same order of magnitude to the wave vector.

As shown by the concrete calculations, in most cases in the calculation of the velocities v_S and v_P the contribution of the nondiagonal terms (formulas (5) and (6) of[2]) of the conductivity tensor σ_{ik} turns out to be small and they can be regarded only as corrections. If we neglect these terms, then the dispersion equation for $(\omega\Omega^{-1}\tan\vartheta)^2 \ll 1$ (formula (12) of[2]) simplifies greatly, breaking up into two equations:

$$\sigma_{xx} + \frac{ic^2}{4\pi\omega}k^2 = 0, \qquad \sigma_{yy} + \frac{ic^2}{4\pi\omega}k^2\cos^2\vartheta = 0, \tag{2}$$

which determine the velocity of the S and P waves, respectively. (The coordinate axes are chosen such that $H \parallel z$, and k lies in the plane of the axes z and y.) From Eq. (2) it follows that $v_P/H \propto \cos\vartheta$ for arbitrary and not only for small values of $\cos\vartheta$. Another important consequence is that the values of $(v_P/H)/\cos\vartheta$ and v_S/H should coincide for identical directions of the magnetic field, but in both cases at mutually perpendicular directions of k. For example, the following should be pairwise equal: a) v_S/H when H is in the C_1C_2 plane and $k \parallel C_3$, and $(v_P/H)/\cos\vartheta$ when H is in the same direction and $k \parallel C_2$ (or $k \parallel C_1$); b) v_S/H when H is in the C_1C_3 plane and $k \parallel C_2$, and $(v_P/H)/\cos\vartheta$ when H is in the same direction and $k \parallel C_3$ (or $k \parallel C_1$); 3) v_S/H when H is in the plane C_2C_3 and $k \parallel C_1$, and $(v_P/H)/\cos\vartheta$ when H is in the same direction and $k \parallel C_3$ (or $k \parallel C_2$). The validity of these equations follows from the fact that when the vector k is rotated through $\pi/2$ the axes x and y interchange places and therefore σ_{xx} and σ_{yy} also interchange places.

1.4. Let us consider the behavior of the P waves at small values of $\cos\vartheta$, when there is no time-dependent dispersion (i.e., $(\omega/\Omega)^2 \ll 1$), but $(\omega\Omega^{-1}\tan\vartheta)^2 \approx 1$. To calculate the velocity of the P wave in this case, it is necessary to take into account in the dispersion equation terms of the type $k_y k_z$. As a result, the value obtained for the wave vector (neglecting the off-diagonal components of the conductivity tensor) is

$$k^2 = \frac{4\pi\omega}{ic^2}\frac{\sigma_{yy}}{\cos^2\vartheta}\left(1 - \frac{\sigma_{yy}\sigma_{zz}}{\cos^2\vartheta}\right)^{-1}, \tag{3}$$

meaning a faster-than-linear increase of k with increasing H^{-1}.

2. EXPERIMENT

The experiments were performed in the frequency range $f \approx 9$–36 GHz, in fields up to 10 kOe, and at a sample temperature $\sim 1.5°$K. The experiment technique is described in detail in[2,3].

In view of the strong dependence of the wave velocity in the direction of the magnetic field, an exact determination of the direction of the magnetic field relative to the crystal axes is of particular importance in the comparison of the results of different experiments. To this end, experiments of three types were performed: a) determination of the symmetry of the wave velocity, b) measurement of the cyclotron resonance, c) observation of the cyclotron resonance at frequencies shifted by the Doppler effect. The direction of the magnetic field, parallel to the surface of the sample, was established by means of the symmetry of the velocity of the P waves at small $\cos\vartheta$ relative to the inclination of the field to the surface of the sample, or by determining the maximum of the amplitude of the cyclotron resonance at the limiting points.

The samples used were single crystals of Bi in the form of discs of 18 mm diameter and 2—0.2 mm thick[1-3], the normal to the flat surface coinciding with the direction of one of the axes (C_1, C_2 or C_3) with accuracy 1—2° (the orientation of the sample was monitored by x-ray diffraction). As shown by the results of the experiments performed with different samples with identical orientation, and also calculations of the wave velocity, such deviations of the direction $k \parallel N$ from the direction of any crystal axis has practically no effect on the wave velocity. We shall therefore assume below that k in each sample is parallel to one of the axes C_1, C_2 or C_3.

The wave propagation in the Bi sample leads to the appearance of resonant absorption of microwave power when standing waves are excited. The maxima of the absorption correspond to satisfaction of the condition $n\lambda/2 = B$(n—number of half waves, D—thickness of sam-

2)In the table we list the quantity v/H, which is the reciprocal of the quantity given in the diagrams of Figs. 1–6 (see below), to facilitate the calculation of the wave velocity.

Direction of **k** and polarization of microwave current	Reference	f, GHz	v/H, 10^4 cm/sec-Oe	Field range	$\frac{\omega}{\Omega}$	$\frac{k\bar{v}_F}{\omega}$	$\frac{k\bar{v}_F}{\Omega}$	$\frac{\pi D}{\lambda}$	Possible correction %
H ∥ C_3									
k ∥ C_3, **J** ∥ C_1 or **J** ∥ C_2		9.35	3.05±0.05	4—10		0.4			—3
		18.92	3.07±0.05	5—10		0.3			—2
	[5]	52.6	1.9; 2.6	4—9	0.35	0.6		0.25	—5
	[7]	~2	2.97; 3.07	4—25		0.4			—3
	Calculation		2,93±0,15						
k ∥ C_1, **J** ∥ C_2		9.47	2,75±0.05	2—10				0,2	<1
		24.85	2.75±0,05	5—10	0,1				<1
	[5]	52.6	2.9	3—9	0.4			0,5	+2
	[6]	13—18	2.38						
	Calculation		2.93±0.15						
k ∥ C_2, **J** ∥ C_1		9.44	3.1±0.15	2—10				0.2	<1
	[4]	~9	2.94	4—7	0.05				<1
	[5]	52.6	2.4	<9	0.14				>1
	[6]	13—18	2.03						
	Calculation		2.93±0.15						
H ∥ C_2									
k ∥ C_2, **J** ∥ C_3		9.27	2.40±0.1	4—10	0.1		0.1		+1
		21.1	2.36±0.1	4—10	0.2		0.2		+4
		27.07	2.24±0.1	6—10	0.15		0.1		+3
		35,86	2.23±0.1	6—10	0.25		0.15		+5
	[4]	~9	2.40	4—7	0.1		0.1		+1
	[5]	52.6	2.30	5—9	0.45		0,4		≈+20
	[7]	~2	2.58	4—25	0.02				<1
	[8]	13—18	2.25 *						
	Calculation		2,50±0.1						
k ∥ C_2, **J** ∥ C_1		9.27	1.90±0.05	4—10	0.15				<1
	[4]	~9	1.71	4—7	0.15				<1
	[5]	52.6	1.92	6—9	0.6				≈+10
	[7]	~2	2.18	4—25	0.03				<1
	[8]	13—18	2.6 *						
	Calculation		2.07±0.08						
k ∥ C_3, **J** ∥ C_1		9.50	1.87±0.05	2—10	0.35			0.1	+5
		21.23	1.81±0.07	5—10	0.30				+5
		24.83	1.74±0.1	4—10	0.45				+10
	[5]	52.6	1.3	<9	>0.4				>10
	[6]	13—18	1.93	5—20	0.3				+5
	Calculation		2.12±0.08						
k ∥ C_3, **J** ∥ C_2		9.53	2.73±0.1 **	≈4—10				≈0.4	≈—5
		18.92	2.54±0.1 ***	~7—10				0.25	≈—2
	Calculation		2.45±0.1 **						
k ∥ C_1, **J** ∥ C_3		9.47	2.30±0.05	2—10	0.2			0.2	<1
		25.0	2.40±0.1	4—10	0.2				+2
	[5]	52.6	2.9	4—9	0.5				+12
	[6]	13—18	2.94						
	Calculation		2.45±0.1						
H ∥ C_1									
k ∥ C_1, **J** = C_{12}	[5]	52.6	~1,3	7—9	0.5		0.1		+15
	[7]	~2	2.03						
	[8]	13—18	2.14	>5	<0.2				<+2
	Calculation		2.12±0.08						
k ∥ C_1, **J** ∥ C_3	[5]	52.6	6.7	2—9	1.7		0.35		+15
	[7]	~2	6.40						
	Calculation		6.09±0.15						
k ∥ C_3, **J** ∥ C_2		9.50	1.99±0.05	2—10	0.35			0.07	<1
		21.23	1.97±0.07	5—8	0.3				<1
		24.85	1.98±0.07	4—10	0.45				<1
	[5]	52.6	1,5	<9	>0.4				~1
	[6]	13—18	1.98						
	Calculation		2.12±0.08						
k ∥ C_3, **J** ∥ C_1		9.60	5.5±0.2 **	2—10	0.35			0.1	~1
	Calculation		6.09±0.15**						
k ∥ C_2, **J** ∥ C_3		9.62	6.15±0.1	2—10	0.35			0.07	<1
		21.10	6.08±0.2	4—10	0.4				<1
		27.07	6.00±0.2	4—10	0.5				<1
		35.86	5.83±0.15	4—10	0.65				<1
	[4]	~9	6.6	3—7	0.2				<1
	[5]	52.6	5.40	2—9	1.8			0.4	—5
	[6]	13—18	5.77	5—25	0.3				<1
	Calculation		6.09±0.15						
k ∥ C_2, **J** ∥ C_1		9.50	1.9±0.1 ***	3—10	0.2			0.4	—6
	Calculation		2.12±0.08 **						

*In [8], the symbols for the directions of the high frequency current relative to the crystal axes in the two noted cases were apparently confused.

**The value of (v/H)/cos ϑ, is given.

***The asymptotic value of (v/H)/cos ϑ, obtained from formula (3), is given.

ple). Since v ∞ H, the oscillations of the absorption are periodic functions H^{-1} with period $\Delta H^{-1} = v/2DfH$. Therefore measurement of the velocity of the magnetoplasma wave reduces essentially to measurement of ΔH^{-1}.

The results of the measurements of the wave velocity are shown in Figs. 1—6, and the results at a field H parallel to one of the symmetry axes of the Bi crystal are listed in the table together with data by other authors and with theoretical values obtained using the ellipsoidal model of the Fermi surface of bismuth.

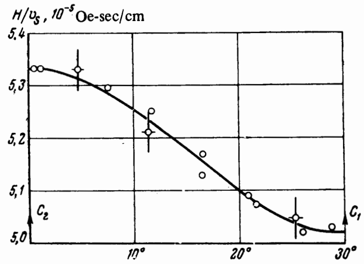

FIG. 1. Anisotropy of the quantity H/v_S at $\mathbf{H}\perp\mathbf{k}\parallel C_3$ and f = 9.5 GHz. The values were obtained within the limits of the rotation of the field through 60°. All the data are reduced to a 30° angle interval. The direction of the axis was determined from the cyclotron resonance. The measurement error is indicated at several points.

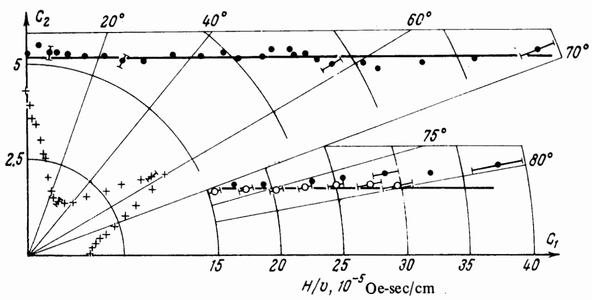

FIG. 2. Anisotropy of the quantity H/v at $\mathbf{H}\perp C_3$, $\mathbf{k}\parallel C_2$, and f = 9.50 GHz: X—$\mathbf{J}\parallel C_3$, S-wave; ●—$\mathbf{J}\parallel C_1$, P-wave; O—obtained with the aid of formula (4). The direction $\mathbf{H}\parallel\mathbf{N}$ was determined accurate to ±10′ from the maximum of the amplitude of the cyclotron resonance of the electrons at the limiting point, and the direction of the crystal axis was determined accurate to ±10′ by cyclotron resonance.

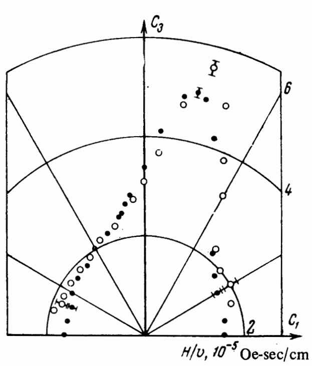

FIG. 3. Anisotropy of H/v at $\mathbf{H}\perp C_2$: ●—$\mathbf{H}\perp\mathbf{k}\parallel C_2$, S-wave, f = 9.44 GHz; O—(H/v) cos ϑ, $\mathbf{k}\parallel C_3$, $\mathbf{J}\parallel C_1$, P wave, f = 9.60 GHz. The directions of the axes were determined accurate to ±1% from cyclotron resonance.

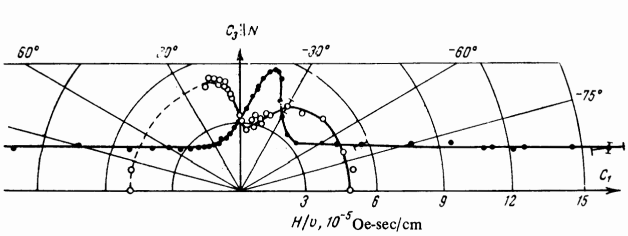

FIG. 4. Anisotropy of H/v at $\mathbf{H}\perp C_2$ and $\mathbf{k}\parallel C_3$: ●—$\mathbf{J}\parallel C_1$, P wave, f = 9.60 GHz; O—$\mathbf{J}\parallel C_2$, S wave, f = 9.35 GHz. The direction $\mathbf{H}\perp\mathbf{N}$ was determined from the symmetry of the picture for P waves at small values of cos ϑ accurate to ± 0.5%, the direction of the C_1 axis accurate to ± 1° from cyclotron resonance, and that of the C_3 axis accurate to ±10′ from the equality of the velocities of both waves.

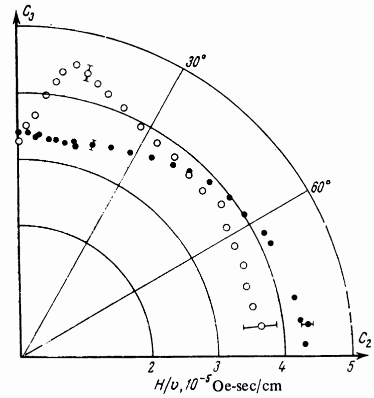

FIG. 5. Anisotropy of H/v at $\mathbf{H}\perp C_1$: ●—$\mathbf{H}\perp\mathbf{k}\parallel C_1$, S wave, f = 9.47 GHz; O—(H/v) cos ϑ, $\mathbf{k}\parallel C_3$, $\mathbf{J}\parallel C_2$, P wave, f = 9.53 GHz. The directions of the axes were determined accurate to ±1° from the symmetry of the picture.

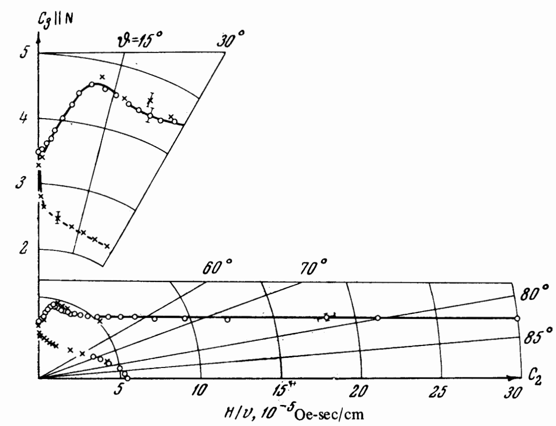

FIG. 6. Anisotropy of H/v at $\mathbf{H}\perp C_1$: O—$\mathbf{J}\parallel C_2$, f = 9.53 GHz; X—$\mathbf{J}\parallel C_1$, f = 9.35 GHz. The direction $\mathbf{H}\perp\mathbf{N}$ was determined accurate to ±0.5° from the symmetry of the picture at small values of cos ϑ, the direction of C_2 accurate to ±0.5° from cyclotron resonance, and the direction of C_3 accurate to ±10′ from the equality of the velocities of both waves.

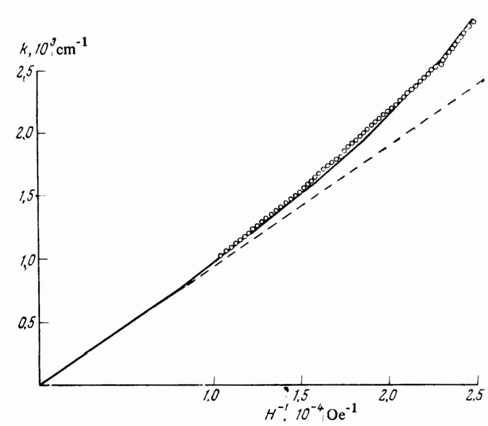

FIG. 7. Dependence of the wave vector of the P wave on H^{-1}; $\mathbf{H}\perp C_3$, $\mathbf{k}\parallel C_2$, $\mathbf{J}\parallel C_1$, ϑ = 73.5°; f = 9.50 GHz. In the construction of the calculated curve (solid line) by formula (4), the value of σ_{yy} was chosen such as to satisfy the experimental data. This value is ~ 4% larger than the value calculated using the ellipsoidal model of the Fermi surface. Dashed line—asymptote as $H^{-1}\to 0$.

To increase the measurement accuracy, it is desirable to determine ΔH^{-1} for the maximum possible range of variation of the magnetic field. In the experiments, the limits of the field were determined such that the deviations of the $k(H^{-1})$ dependence from linear did not exceed the measurement error. Violations of the periodicity of the oscillations were due to the following causes.

In strong fields they were due to the influence of quantum effects on the change of the Fermi level, and by the same token on the wave velocity. However, the quantum effects were small even in the maximum field ~ 10 kOe of the magnet employed by us (see, for example, the deviations of the experimental points from the calculated curve in Fig. 7).

In weak fields, temporal and spatial dispersion appeared, leading to the appearance of additions to the components of the conductivity tensor, of the order of $(\omega/\Omega)^2$, $(\mathbf{k}\cdot\overline{\mathbf{V}}_F/\omega)^2$, $(\mathbf{k}\cdot\overline{\mathbf{V}}_F/\Omega)^2$, and $(\pi d/\lambda)^2$. The table lists the maximum values of those parameters whose influence are the difference between the wave velocity and the asymptotic value is most appreciable. Concrete calculations show that the appearance of dispersion does not always effect the wave velocity strongly. Therefore, in order to assess the possible systematic difference between the measured values of v/H and the asymptotic ones, the last column of the table lists an estimate of the addition to the velocity due to the temporal and spatial dispersions.

3. DISCUSSION OF RESULTS

3.1. We shall investigate first the relations between the velocities of the S and P waves. According to Fig. 1, the velocity v_S with $\mathbf{k} \parallel C_2$ and $H \perp C_3$ changes only by ~ 7% when the field is rotated from the C_2 axis to C_1. The points for H/v_P at $\mathbf{k} \parallel C_2$ and for H in the basal plane fit a straight line on the polar diagram of Fig. 2, within the limits of measurement accuracy, thus indicating that the quantity $(v_P/H)/\cos\vartheta$ is isotropic in this plane. The values of v_P/H and v_S/H at $H \parallel C_2$ coincide for these two cases, in accordance with the table.

The values of v_S/H with $\mathbf{k} \parallel C_2$ and $H \perp C_2$ and of $v_P/H)/\cos\vartheta$ with $\mathbf{k} \parallel C_3$ and $H \perp C_2$ are shown in Fig. 3; this figure demonstrates the practically complete agreement of the two groups of experimental points.

In the case $H \perp C_1$, according to Fig. 5, there is a noticeable difference between v_S/H at $\mathbf{k} \parallel C_1$ and $(v_P/H)/\cos\vartheta$ at $\mathbf{k} \parallel C_3$ when the direction of the field H is close to the trigonal axis. It can be shown that at such a field configuration σ_{xy} has the same order of magnitude as σ_{xx} and σ_{xy}; in particular, if the angle between H and C_3 is ≈7°, when H is perpendicular to the major axis (αaxis) of one of the electronic ellipsoids, we have $\sigma_{xx} \approx \sigma_{yy}$ and $\sigma_{xy} \approx \sigma_{yy}/\sqrt{3}$. Calculation shows that when $\mathbf{k} \parallel C_3$ there should be excited waves with two velocities: $v_P/H = (2.4 \pm 0.1) \times 10^4$ cm/sec-Oe and $v_S/H = (4.16 \pm 0.4) \times 10^4$ cm/sec-Oe, and when $\mathbf{k} \parallel C_1$ the velocity of the S wave is $v_S/H = (3.45 \pm 0.4) \times 10^4$ cm/sec-Oe. The experiments yield the following respective values: $v_P/H = (2.35 \pm 0.15) \times 10^4$ cm/sec-Oe, $v_S/H = (4.0 \pm 0.15) \times 10^4$ cm/sec-Oe when $\mathbf{k} \parallel C_3$, and $v_S/H = (3.0 \pm 0.1) \times 10^4$ cm/sec-Oe when $\mathbf{k} \parallel C_1$, which shows the agreement between them within the limits of the calculation and experimental errors.

We have thus confirmed experimentally the relations established in Sec. 1.3 between the velocities of the S and P waves, for which knowledge of the exact model of the Fermi surface is not required in practice (it is sufficient to have a rough idea of the model in order to obtain estimates of the different components of the conductivity tensor).

3.2. According to experiment, in the case $\mathbf{k} \parallel C_2$ and $H \perp C_3$ and at low values of $\cos\vartheta$, $k(H^{-1})$ dependence for the P wave differs noticeably from linear (Fig. 7). Estimates show that in the region of fields in which the P waves are observed, the inequalities $(\omega/\Omega)^2 \lesssim 3 \times 10^{-2}$ and $(\mathbf{k}\cdot\overline{\mathbf{V}}_F/\omega)^2 \lesssim 10^{-2}$ are satisfied. Therefore, in calculating the components of the conductivity tensor it is possible to confine oneself to their asymptotic values, i.e., the temporal and the spatial dispersion are negligibly small. However, in solving the dispersion equation it is necessary to take into account terms of order $(\omega\Omega^{-1}\tan\vartheta)^2 \approx 0.4$; in this case the value of k is determined by formula (3), which then assumes the form

$$k^2 = \frac{4\pi\omega}{ic^2}\frac{\sigma_{yy}}{\cos^2\vartheta - \omega^2/\Omega^2}. \quad (4)$$

The curve determined by this expression is shown in Fig. 7. In its calculation, σ_{yy} was chosen such as to obtain best agreement with experiment; this value turns out to be ~ 4% larger than that calculated on the basis of the ellipsoidal model.

The fact that k increases more rapidly than H^{-1} for P waves is reflected in the diagram of Fig. 2, which shows the values of H/v for P waves, obtained both from formula (4) and from the oscillation period ΔH^{-1}, determined directly from experiment at $H \lesssim 10$ kOe. In the second case, the values of H/v turn out to be larger, corresponding to a period ΔH^{-1} which is smaller than in the asymptotic case. Such a behavior agrees with Fig. 7. We note that the asymptotic values of H/v, up to an angle $\vartheta \approx 80°$, lie on a straight line corresponding to the change of ΔH^{-1} in accordance with the law $\Delta H^{-1} \propto \cos\vartheta$, i.e., to the spectrum of the wave $\omega \propto \mathbf{k}\cdot\mathbf{H}$.

It is seen from the diagrams of Figs. 4 and 6 that in the case when $\mathbf{k} \parallel C_3$, $H \perp C_1$, or $H \perp C_2$, at small values of $\cos\vartheta$, the experimental points lie on straight lines, i.e., no difference is observed between the period ΔH^{-1} and its asymptotic value. Such a behavior agrees with the theory, since when $\mathbf{k} \parallel C_3$ and $H \perp C_2$ it turns out that

$$k^2 = \frac{4\pi\omega}{ic^2}\frac{\sigma_{yy}}{\cos^2\vartheta}\left[1 - \left(\frac{\omega}{\Omega}\operatorname{tg}\vartheta\right)^2\frac{M_1}{M_3}\right]^{-1},$$

and $M_1/M_3 \approx 0.1$, so that the second term in the square bracket can be neglected. When $H \perp C_1$ and $\mathbf{k} \parallel C_3$, the spectrum of the wave is determined by the electrons, for which the value of $(\omega\Omega^{-1}\tan\vartheta)^2$ at the same values of H and ϑ is smaller by a factor of approximately 4. When the frequency is doubled (from ~ 9.5 to ~ 18.9 GHz), allowance for the difference between the dependence of the wave velocity on the field from linearity becomes essential; accordingly, the asymptotic value of v/H listed in the table for this case has been calculated in accordance with formula (3).

3.3. Let us consider the values of v/H when H and k are parallel to the symmetry axis of the bismuth crystal. When $H \parallel C_3$, regardless of the direction of k, the velocities of both waves should coincide, owing to symmetry requirements. Such an equality is indeed observed when $\mathbf{k} \parallel C_3$ and $\mathbf{k} \parallel C_2$. When $\mathbf{k} \parallel C_1$, the value of v/H turns out to be somewhat smaller, and this is possibly connected with the error in the orientation of the field; such a difference can appear when the field is inclined at an angle ~ 1–2° to the plane containing the axes C_2 and C_3 (this is seen from the diagram in Fig. 3).

As indicated in Sec. 1.3, the off-diagonal components in the conductivity tensor are as a rule negligibly small. According to estimates based on formula (7) of[2], using an ellipsoidal model of the Fermi surface and **H** and **k** directed along the axes C_1, C_2, or C_3, allowance for these components can lead to a correction not exceeding ~ 1–2% of the velocity. The values of v_S/H and $(v_P/H)/\cos\vartheta$ should coincide therefore with the same accuracy, under the following conditions:

(a) when $\mathbf{H}\parallel C_2$ for the cases $\mathbf{k}\parallel C_2$, $\mathbf{J}\parallel C_3$; $\mathbf{k}\parallel C_1$, $\mathbf{J}\parallel C_2$ and $\mathbf{k}\parallel C_3$, $\mathbf{J}\parallel C_2$;
(b) when $\mathbf{H}\parallel C_2$ for the cases $\mathbf{k}\parallel C_2$, $\mathbf{J}\parallel C_1$ and $\mathbf{k}\parallel C_3$, $\mathbf{J}\parallel C_1$;
(c) when $\mathbf{H}\parallel C_1$ for the cases $\mathbf{k}\parallel C_3$, $\mathbf{J}\parallel C_2$ and $\mathbf{k}\parallel C_2$, $\mathbf{J}\parallel C_1$;
(d) when $\mathbf{H}\parallel C_1$ for the cases $\mathbf{k}\parallel C_3$, $\mathbf{J}\parallel C_1$ and $\mathbf{k}\parallel C_2$, $\mathbf{J}\parallel C_3$.

(We do not present here all the possible situations, but only those investigated in our experiments.) The corresponding values do agree within the limits of measurement error, as can be seen from the table.

According to[11], the hole surface has axial symmetry with respect to the C_3 axis, with accuracy ~ 1%. Therefore the velocities of the S waves determined by the holes should agree when $\mathbf{k}\parallel C_3$ and $\mathbf{H}\parallel C_2$ or $\mathbf{H}\parallel C_1$. Allowance for the electrons, which make a contribution of ~ 2%, does not change the situation, since the additions are equal in both cases. At the same time, according to experiment, the S-wave velocity has an anisotropy amounting to ~ 7% (see Fig. 1). Such a behavior can apparently be attributed to the influence of the temporal dispersion, which leads in the case of $\mathbf{H}\parallel C_2$ to a deviation of ~ 5% from the asymptotic velocity, i.e., a deviation of the same order of magnitude as the observed anisotropy.

3.4. The numerical values of the wave velocities measured in the present paper coincide, within the limits of the experimental and computational errors, with the theoretical values obtained using the ellipsoidal model of the Fermi surface with the parameters given in Sec. 1.2.

The table lists, besides the values of v/H measured and calculated by us, also wave-velocity data obtained by others. The results of Kirsch[4] and McLachlan[7] practically coincide with ours, and the agreement with the results of Smith and Williams[8] is good enough if it is assumed that they confused the current polarization directions at $\mathbf{H}\parallel C_2$ and $\mathbf{k}\parallel C_2$.

Appreciable discrepancies occur when a comparison is made with the results of Faughnan[5]. However, as shown by estimates, the results of[5] were obtained in a region where it is already necessary to take dispersion into account, but this was not done by Faughnan. Another no less important shortcoming of his investigation is the presence of large errors in the determination of the orientation of the magnetic field relative to the crystal axes. This is evidenced, in particular, by the difference between the values of the velocities of the S and P waves when $\mathbf{H}\parallel C_3$ and $\mathbf{k}\parallel C_3$ (see the table), a difference that can be attributed only to the fact that **H** is not parallel to C_3.

The appreciable quantitative discrepancies between our results and those of Williams[6] at $\mathbf{H}\parallel C_3$ can be apparently ascribed to errors in the determination of the directions of the magnetic field in[6]; it is difficult to think of other causes, since it is impossible to determine from[6] the field range in which the measurements were performed. In any case, we can see no other grounds for the difference between our velocities and those obtained by Williams, all the more since the frequencies employed by him, ~ 13–18 GHz, fall in the range ~ 9–36 GHz employed by us.

CONCLUSION

The foregoing analysis shows that the theory describes qualitatively the properties of the magnetoplasma waves in Bi. When the ellipsoidal model of the Fermi surface is used for Bi, with parameters obtained from other experiments[11-14], agreement is obtained (within the limits of the measurement and calculation errors) between the experimentally measured and calculated values of the magnetoplasma wave velocities.

Of great importance in the comparison of the results of the experiments performed at different frequencies is allowance for the temporal and spatial dispersion. In any case, it is even necessary, when finding the asymptotic values of the velocities, to see to it that the experiment is performed at field values in which there is no dispersion, or else to introduce a suitable correction for the change in the wave velocity. Neither of these requirements is satisfied by Faughnan[5], so that his results cannot be at all compared with our experiments or with those by others without an indication of the exact limits of the magnetic field at which they were obtained.

If we disregard the results obtained by Williams[6] at $\mathbf{H}\parallel C_3$, assuming that the differences are due only to the errors made in the determination of the field orientation, and if we disregard Faughnan's data[5], then the results obtained in the frequency range 2–36 GHz are in agreement (see the table). Thus, at least in this frequency range, the properties of magnetoplasma waves are in satisfactory agreement with the theory.

In view of the fact that the wave velocity is an integral characteristic of the carrier spectrum in Bi, it is practically impossible to establish the form of the Fermi surface by investigating the plasma waves in the asymptotic region with the same accuracy as by means of experiments on cyclotron resonance, cyclotron resonance cutoff, and quantum oscillations[11-14]. It is, however, possible to obtain the total number of electron and hole ellipsoids per reciprocal-lattice cell. According to the present paper, their number is respectively 3 and 1. It can also be stated that there are no other sections of the Fermi surface having an appreciable value, and all the more, that there are no "heavy carriers" whose contribution to the wave velocity might be large.

The author thanks P. L. Kapitsa for interest in the work, M. S. Khaĭkin for a discussion and valuable advice, and G. S. Chernyshev and V. A. Yudin for technical help.

[1] M. S. Khaĭkin, R. T. Mina, and V. S. Edel'man, Zh. Eksp. Teor. Fiz. **44**, 2190 (1963) [Sov. Phys.-JETP **17**, 1470 (1963)].

[2] M. S. Khaĭkin, L. A. Fal'kovskiĭ, V. S. Édel'man, and R. T. Mina, ibid. **45**, 1704 (1963) [**18**, 1167 (1964)].

[3] M. S. Khaĭkin and V. S. Édel'man, ibid. **49**, 1695 (1965) [**22**, 1159 (1966)].

[4] J. Kirsch, Phys. Rev. **133**, A1390 (1964).

[5] B. W. Faughnan, J. Phys. Soc. Japan **20**, 574 (1965).

[6] G. A. Williams, Phys. Rev. **139**, A771 (1965).

[7] D. S. McLachlan, Phys. Rev. **147**, 368 (1966).

[8] G. E. Smith and G. A. Williams, IBM J. Res. and Dev. 8, 276 (1964).

[9] S. J. Buchsbaum and J. K. Galt, Phys. Fluids **4**, 1514 (1961).

[10] É. A. Kaner and V. G. Skobov, Zh. Eksp. Teor. Fiz. **45**, 610 (1963) and **46**, 1106 (1964) [Sov. Phys.-JETP 18, 419 (1964) and **19**, 749 (1964)].

[11] V. S. Édel'man and M. S. Khaĭkin, ibid. **49**, 107 (1965) [**22**, 77 (1966)].

[12] M. S. Khaĭkin and V. S. Édel'man, ibid. **47**, 878 (1964) [**20**, 587 (1965)].

[13] M. S. Khaĭkin, V. S. Édel'man, and R. T. Mina, ibid. **43**, 2063 (1962) [**16**, 1459 (1963)].

[14] N. B. Brandt, T. F. Dolgolenko, and N. N. Stupochenko, ibid. **45**, 1319 (1963) [18, 908 (1964)].

Translated by J. G. Adashko
201